

## Influence of rare gases on cavity formation at indium impurities in copper

R. Schumacher and R. Vianden

*Institut für Strahlen- und Kernphysik der Universität Bonn, D-5300 Bonn, Federal Republic of Germany*

(Received 23 March 1987)

The interaction of implanted gases such as He, Ne, Ar, Kr, and Xe with substitutional indium impurities in copper has been studied by the time-differential perturbed angular correlation technique. In spite of the very different size of the gas atoms, in all cases identical electric field gradients were observed at the indium site. It is shown that the gas implantation initiates the growth of large cavities at the indium impurity and the observed electric field gradient is due to indium atoms situated at the inner surface of the cavities. The influence of the gas atoms inside the cavities on the observed electric field gradient can be neglected.

### I. INTRODUCTION

Helium in metals is known to cause severe changes in their properties as, e.g., loss of ductility, swelling, and diminished crack resistance. These phenomena are of great importance for the design and operation of components in the fission and fusion energy technology where helium is introduced into metals by nuclear transmutation processes or direct implantation of  $\alpha$  particles.

In unstressed components and in the simultaneous presence of radiation-induced vacancies the dominating effect is swelling caused by the formation of three-dimensional clusters of vacancies, usually called cavities. The influence of helium and other gases on the formation of these cavities has been studied. The experimental work has been reviewed recently by Farrell.<sup>1</sup> However, little is known about the role played by substitutional impurities in the early stages of nucleation and growth of these cavities.

Nuclear techniques like the Mössbauer effect or time-differential perturbed angular correlation (TDPAC) have been very successful in the study of intrinsic defects in metals.<sup>2,3</sup> Because of the extreme sensitivity of these methods to the charge distribution in the immediate vicinity of the probe atom, they seem also well suited for studying the early stages of radiation-induced cavity growth.

In copper, the interaction of vacancies with substitutional <sup>111</sup>In has been studied extensively by use of the TDPAC technique.<sup>4</sup> In the temperature range of recovery stage III, two different indium-defect configurations were found. They were identified as a monovacancy and a divacancy trapped at the probe atom, respectively. The interpretation of a third defect configuration appearing in recovery stage V remained controversial since a planar faulted loop as well as a stacking fault tetrahedron have been suggested to explain the observed properties of this defect.<sup>4,5</sup> In further TDPAC experiments the interaction of implanted helium with these probe-atom-defect complexes has been studied.<sup>6,7</sup> However, here also some questions regarding the configuration of the resulting complex remained.

In the present paper we report on TDPAC measurements where the effects of implanted He, Ne, Ar, Kr, and Xe as well as N were investigated under identical conditions. The results shed new light on the influence of interstitial gases and substitutional impurities on the formation of cavities in metals and allow a consistent interpretation of the previously obtained TDPAC results in copper.

### II. EXPERIMENTAL DETAILS

#### A. The $\gamma$ - $\gamma$ TDPAC technique

The  $\gamma$ - $\gamma$  TDPAC technique used in this investigation is based on the observation of the interaction of a defect-induced electric-field-gradient (EFG) tensor, described by its main component  $V_{zz}$  and the asymmetry parameter  $\eta = (V_{xx} - V_{yy})/V_{zz}$ , and the nuclear quadrupole moment ( $Q$ ) of the probe nucleus. The interaction leads to a change in the directional correlation of two  $\gamma$  rays emitted successively by the probe nucleus. This correlation was observed by taking time-differential coincidence spectra for 90° and 180° with a setup of four 51  $\phi \times 51$  mm CsF detectors, mounted in a plane around the sample. Energy and time information was derived from the anode signals of the photomultipliers by use of window constant fraction discriminators. The time resolution reached with this setup was typically 1.2 nsec (FWHM) for the 172–247 keV  $\gamma$ - $\gamma$  cascade emitted in the decay of <sup>111</sup>In. From the coincidence counting rates  $W_{ik}(\theta, t)$  ( $\theta = 90^\circ, 180^\circ$ ;  $i$  and  $k$  denote number of detectors), the standard four-detector asymmetry ratio<sup>8</sup>

$$R(t) = 2[W(180^\circ, t) - W(90^\circ, t)] / [W(180^\circ, t) + 2W(90^\circ, t)],$$

with

$$W(180^\circ, t) = [W_{13}(180^\circ, t)W_{24}(180^\circ, t)]^{1/2}$$

and

$$W(90^\circ, t) = [W_{23}(90^\circ, t)W_{14}(90^\circ, t)]^{1/2}$$

was evaluated.  $R(t)$  is equal to  $A_{22}G(t)$ , where  $A_{22}$  is

the lowest-order directional correlation coefficient of the  $\gamma$ - $\gamma$  cascade and  $G(t)$  is the time-dependent perturbation function. It contains information about the quadrupole interaction. The data taken in this way were analyzed assuming a theoretical perturbation function of the form

$$G(t) = \sum_{n=0}^3 s_n(\eta) \cos[c_n(\eta)v_Q t].$$

$v_Q = eQV_{zz}/h$  is the quadrupole-interaction (QI) frequency.  $c_n(\eta)$  are well-known functions of  $\eta$ . For polycrystalline samples with randomly oriented EFG's, the  $s_n(\eta)$  depend only on  $\eta$  and are independent of the orientation of the detectors relative to the sample. For probe atoms in a single crystal the  $s_n$  depend additionally on the orientation of the EFG tensor, represented by its values  $V_{zz}, V_{yy}, V_{xx}$  ( $V_{zz} \geq V_{yy} \geq V_{xx}$ ) along the principal axes, within the crystal and on the position of the crystal axes with respect to the  $\gamma$ -ray detectors. From the changes in the perturbation patterns for different alignments of the detectors along the main crystal axes ( $\langle 100 \rangle, \langle 110 \rangle, \langle 111 \rangle$  in our experiment) one can derive the orientation of the EFG's principal axes relative to the crystallographic axes. A detailed description of the method has been given by Wegner.<sup>9</sup>

### B. Sample preparation

Cu foils of 25- $\mu\text{m}$  thickness and a purity of 99.999% were used in our experiments. Before the implantation the foils as well as the Cu single crystal were etched in 10%  $(\text{NH}_4)_2\text{S}_2\text{O}_8$  and the foils were annealed under vacuum ( $p \leq 10^{-7}$  kPa) for 30 min at 1073 K.

All implantations were carried out at the Bonn isotope separator with the sample kept at room temperature.  $^{111}\text{In}$  was implanted with 80 keV and typical doses of  $(2-4) \times 10^{13}$  atoms/cm<sup>2</sup>. After annealing the sample in vacuum for 10 min at 523 K (the choice of this temperature will be explained below) the gas implantations were carried out again at room temperature. Here the dose was  $2 \times 10^{14}$  atoms/cm<sup>2</sup> and the implantation energy was chosen appropriately to create a good overlap between the indium probe ions and the postimplanted gas (Fig. 1).

The Cu single crystal was implanted in a tilted position in order to avoid channeling of the incoming indium

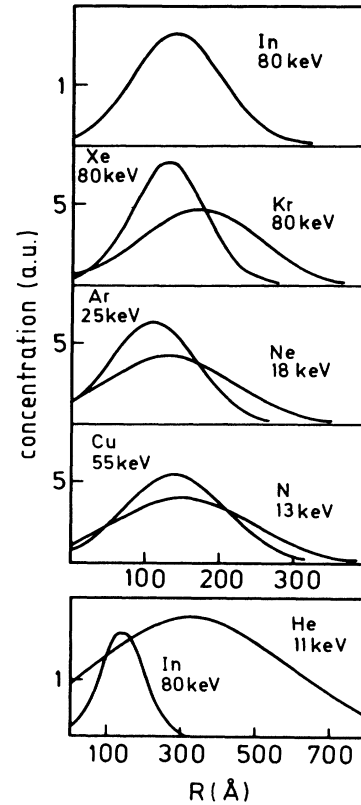


FIG. 1. Implantation energies and estimated range distributions for different implants in copper.

or gas ions. Isochronous annealing steps of the gas-implanted samples were carried out in vacuum ( $p \leq 10^{-6}$  kPa) with a holding time of 10 min. All TDPAC measurements were carried out at room temperature.

### III. RESULTS

After the implantations and each annealing step TDPAC spectra were recorded with the four-detector CsF setup. The above-mentioned asymmetry ratios were formed and a theoretical perturbation function was fitted to the data by the least-squares method. The fit function took into account five different fractions:

$$R(t) = A_{22} \left\{ f_0 + \sum_{i=1}^3 f_i \sum_{n=0}^3 s_n(\eta_i) \cos[c_n(\eta_i)v_{Q_i}t] \exp[-c_n(\eta_i)v_{Q_i}\delta_i t] + f_4 \sum_{n=0}^3 s_n \exp(-n\delta_4 t) \right\}$$

with  $\sum_{i=0}^4 f_i = 1$ .  $f_0$  is the fraction of probe atoms on unperturbed lattice sites, and  $f_i$  ( $i=1,3$ ) are the fractions of probe atoms experiencing quadrupole interactions leading to interaction frequencies  $v_{Q_i}$  with a possible Lorentzian distribution with a half width at half maximum  $\delta_i$  and asymmetry parameters  $\eta_i$ .  $f_4$  is the fraction of probe atoms on sites with only weak EFG's, i.e.,  $v_{Q_4} = 0$  MHz and width  $\delta_4$ .

Before any gas postimplantation the interaction of va-

cancies with implanted In probe atoms in pure copper was studied. In this experiment all conditions, namely the foil preparation, implantation, and annealing parameters were kept equal to those of the following measurements. A fit to the data taken immediately after the implantation gave  $f_4 = 72\%$ , i.e., 72% of the probe atoms are on substitutional sites with only weak perturbations. The remaining fraction is subjected to high but nonunique EFG's caused by different defect

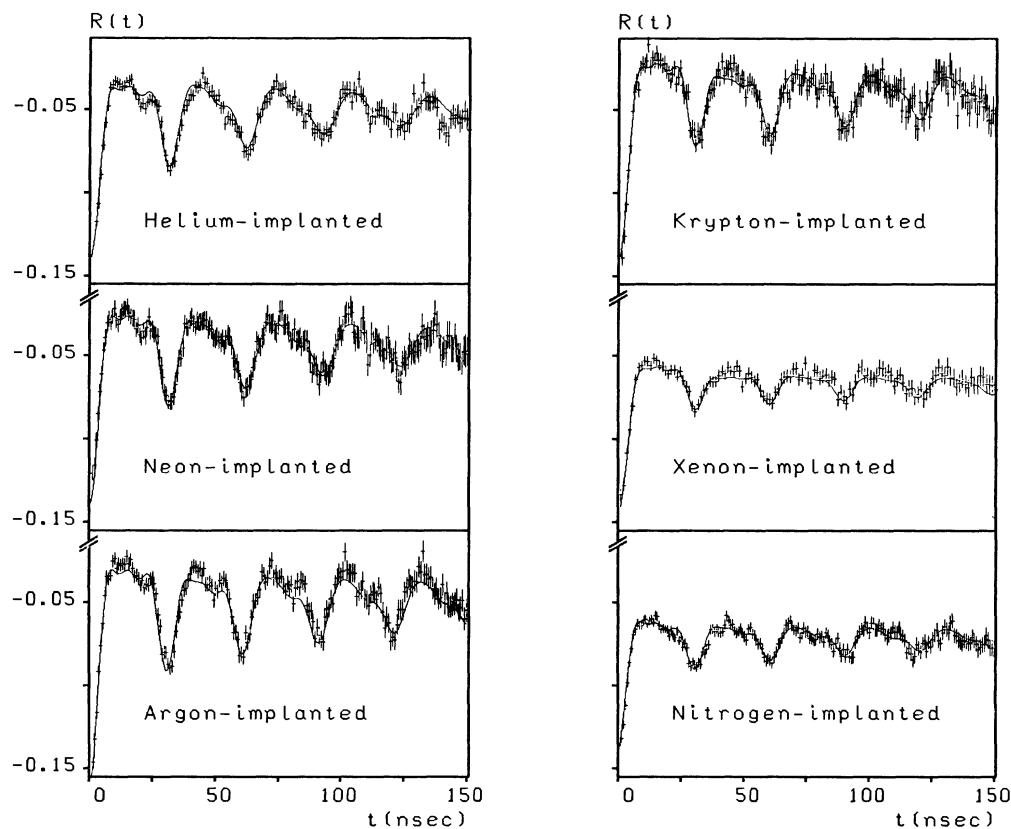


FIG. 2. TDPAC spectra observed for  $^{111}\text{In}$  in copper after implantation of different gases and annealing at 523 K.

configurations in the immediate surrounding of the In atoms. Upon annealing at  $T_{\text{ann}}=373$  K a frequency  $\nu_{Q1}=49.5(7)$  MHz ( $\eta_1=0$ ) appears. The corresponding fraction  $f_1$  reaches a maximum of 10% around  $T_{\text{ann}}=523$  K before it vanishes at  $T_{\text{ann}}=723$  K. In a similar experiment, where the Cu foil after annealing at 523 K (maximum of  $f_1$ ) is implanted with He [Fig. 2(a)], a new well-defined QI frequency  $\nu_{Q2}=208(5)$  MHz ( $\eta_2=0.20$ ) appears. Its fraction  $f_2$  reaches a maximum of more than 50% around  $T_{\text{ann}}=500$  K and decreases slowly to 36% at  $T_{\text{ann}}=703$  K. During the annealing program  $\nu_{Q2}$  increases by about 8% to 223(5) MHz at  $T_{\text{ann}}=703$  K, while the correlated  $\eta_2$  decreases to 0.08.

A surprising result was found if instead of He another

rare gas like Ne, Ar, Kr, or Xe was postimplanted with all other parameters kept unchanged. In each case identical interaction patterns were observed [Fig. 2(b)–(e)] and the least-squares fits yielded the QI frequencies listed in Table I. Isochronous annealing of the samples led to variations in  $\nu_{Q2}$  and  $\eta_2$  as described above, and the fractions  $f_2$  changed as shown in Fig. 3.

A further experiment revealed that even the postimplantation of a nonrare gas like nitrogen led to the same value of the QI frequency [Fig. 2(f) and Table I].

In order to exclude the possibility that these results are only due to the postimplantation process, e.g., caused by the recoil implantation of some surface contamination on the copper foil, a control experiment was

TABLE I. Quadrupole-interaction parameters after implantation of different gases and annealing at the temperature indicated in the last column. The values were obtained from least-squares fits to the data shown in Fig. 2.

Implant	$\nu_{Q2}$ (MHz)	$\eta_2$	$\delta_2$	$f_2$ (%)	$T_{\text{ann}}$ (K)
He	220(5)	0.13(2)	0.074(9)	54(2)	523
Ne	215(5)	0.16(2)	0.070(5)	50(2)	523
Ar	220(5)	0.14(2)	0.054(5)	50(3)	523
Kr	222(5)	0.13(3)	0.068(6)	48(1)	573
Xe	226(6)	0.10(5)	0.081(23)	19(2)	623
N	224(5)	0.13(2)	0.07(1)	23.5(8)	623

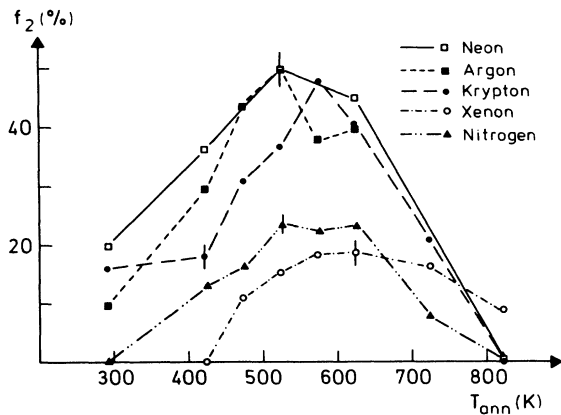


FIG. 3. Fraction of  $^{111}\text{In}$  probe atoms in copper showing the unique quadrupole-interaction frequency  $\nu_{Q2}$  after implantation of different gases (see inset) vs annealing temperature.

carried out by postimplanting Cu. However, in this case the same implanted dose of Cu ions produced only the well-known frequency  $\nu_{Q1}=49.5(7)$  MHz mentioned above.

The orientation of the main component of the EFG tensor leading to  $\nu_{Q2}$  was determined by implanting a copper single crystal with  $^{111}\text{In}$  and postimplanting argon. By comparing the TDPAC patterns obtained for different orientations of the crystal between the detectors to theoretically calculated patterns<sup>9</sup> a  $\langle 111 \rangle$  orientation of  $V_{zz}$  was derived.

#### IV. DISCUSSION

The interaction of defects with indium impurities in pure copper has been studied previously by several groups.<sup>10,11</sup> The present results are in good agreement with the values reported there. Similarly the effects caused by the postimplantation of helium have been investigated.<sup>6,7</sup> Also no discrepancies with the present data were found in the annealing temperature range studied.

Mainly due to its annealing behavior and dose dependence the EFG producing defect configuration in pure copper was thought to be a faulted dislocation loop formed at the indium impurity.<sup>10,11</sup>

As an explanation of the pronounced changes in the QI frequency observed after the helium implantation the formation of small helium-filled vacancy clusters containing two to three vacancies and helium atoms trapped at the substitutional indium probe was suggested.<sup>6,7</sup> However, no definite cluster configuration could be deduced and the explanation of the uniqueness of the observed QI frequency as well as the small, but not negligible, asymmetry parameter  $\eta$  and the measured  $\langle 111 \rangle$  orientation of the main EFG component  $V_{zz}$  remained unsatisfactory.

A further problem arises if one tries to explain the present results in this concept, since the size of the implanted gases differs considerably from He to Xe. Baskes *et al.*<sup>12</sup> have shown that, e.g., in the very similar fcc Ni lattice the interaction energy of rare gases with

vacancies differs by a factor of 3–5 from He to Xe. Further, for rare gases on interstitial positions they expect a completely different behavior depending on the size of the gas atom. On the other hand, it is known that due to its  $1/r^3$  dependence the EFG at the site of the indium nucleus is extremely sensitive to small shifts in the charge distribution around the probe nucleus. Therefore in order to explain the present results one has to assume that the trapping of such differently behaving gas species produces identical changes in the local host lattice symmetry, an idea which makes the above-mentioned concept very implausible.

The independence of the defect-produced EFG on the size of the implanted gas atoms makes it rather probable that the gas atoms only participate catalytically in the formation of a defect complex at the indium probe atom without contributing to the EFG. A possible configuration satisfying this condition would be a larger vacancy cluster (cavity) at the probe atom.

The experimental data about the role of gases in the nucleation of such cavities have been reviewed by Farrell.<sup>1</sup> For the fcc metal Al transmission electron microscopy investigations suggest that under irradiation and in the presence of high argon or xenon concentrations in general, large bubbles of octahedral shape bounded by  $\langle 111 \rangle$  planes are formed.<sup>13</sup> The present experiments now indicate that in pure copper migrating vacancies are trapped at indium and form faulted dislocation loops. If helium or another rare gas is implanted, its interaction with the existing loops initiates and stabilizes the three-dimensional growth of the vacancy agglomerate with the final result of a cavity. The necessary vacancies originate from the implantation process and are released from other traps during the annealing procedure. The indium probe atom initially occupying a site in the central region of the dislocation loop will then find itself situated in the inner  $\langle 111 \rangle$  surface of the cavity. The gas atoms which enabled its growth will finally move freely in the cavity without having any further influence on the measured EFG.

In this picture one can immediately understand the  $\langle 111 \rangle$  direction of the main EFG component  $V_{zz}$  since in a  $\langle 111 \rangle$  surface one expects the gradient of the electric field to be perpendicular. The smallest regular octahedron which possesses a site in a  $\langle 111 \rangle$  surface not directly on an edge or a corner of the octahedron consists of six vacancies. Thus the size of the smallest cavities leading to the observed QI frequency can be estimated to be of the order of 0.4 nm. The slight spread ( $\delta_2$ ) of  $\nu_{Q2}$  and the larger  $\eta_2$  values observed at low annealing temperatures have to be attributed to distant lattice damage and irregularities in the shape of the cavities, respectively. The gradual reduction of  $\eta_2$  and the correlated slight increase of  $\nu_{Q2}$  with increasing annealing temperature would be due to the growth of the cavity which moves the edges of the octahedron further away, thus reducing the asymmetry of the surface EFG. The variation of the maximum fraction  $f_2$  (Fig. 3) for different gases has to be attributed most probably to the slightly different overlap of the implantation profiles (Fig. 1) and the correlated vacancy distributions.

Finally the observation of de Waard *et al.*,<sup>14</sup> who found in a TDPAC experiment in Ni that only a small number (1–2) of He atoms are needed per In probe to create a similar defect EFG, can be understood. It should be mentioned here that the mechanism by which this low number of gas atoms stabilize the cavity could be the pressure it exerts on the walls of the cavity. A rough estimate using the kinetic gas theory yields a value of 50 MPa for one He atom at 293 K in a cavity consisting of six vacancies.

The conclusions drawn above are also in excellent agreement with the experimental results of Schatz *et al.*<sup>15</sup> This group studied the EFG experienced by isolated <sup>111</sup>In atoms evaporated onto clean (100), (110), and (111) copper surfaces. All parameters of the EFG observed for <sup>111</sup>In in a copper (111) surface agree very well with the present results. Small variations in the absolute value of  $\nu_{Q2}$  are explained by varying strains in the copper single crystals produced by different methods.<sup>15</sup> Also the temperature dependence of the surface EFG (Ref. 15) and the helium-induced EFG have been found

to be identical.<sup>16</sup>

In view of these results one can draw some further conclusions. Helium-induced cavity growth<sup>1</sup> and EFG's attributed to decorated defects<sup>6,17,18</sup> have also been observed in several other metals. In gold, the only case where a corresponding surface EFG was measured,<sup>15</sup> two identical QI frequencies are also present. This makes it probable that in the future it will be possible to also study in these metals the early stages of gas-assisted cavity growth at impurities.

Finally this observation of the EFG on inner surfaces will greatly facilitate studies of the general properties of surface EFG's under clean conditions since no influence of adsorbed gas layers which usually build up even under the best ultrahigh vacuum (UHV) conditions has to be expected in cavities.

#### ACKNOWLEDGMENT

This work was funded by the German Federal Minister for Research and Technologie (BMFT) under Contract No. BO1BON.

<sup>1</sup>K. Farrell, *Radiat. Eff.* **53**, 175 (1980).

<sup>2</sup>F. Pleiter and C. Hohenemser, *Phys. Rev. B* **25**, 106 (1982).

<sup>3</sup>E. Bodenstedt, *Hyp. Int.* **24**, 889 (1985).

<sup>4</sup>O. Echt, E. Recknagel, A. Weidinger, and Th. Wichert, *Z. Phys. B* **32**, 59 (1980).

<sup>5</sup>G. Lindner (private communication).

<sup>6</sup>F. Pleiter, A. R. Arends, and H. de Waard, *Phys. Lett.* **77A**, 81 (1980).

<sup>7</sup>M. Deicher, G. Grübel, W. Reiner, and Th. Wichert, *Hyp. Int.* **15/16**, 467 (1983).

<sup>8</sup>A. R. Arends, C. Hohenemser, F. Pleiter, H. de Waard, L. Chow, and R. M. Suter, *Hyp. Int.* **8**, 191 (1980).

<sup>9</sup>D. Wegner, *Hyp. Int.* **23**, 179 (1985).

<sup>10</sup>K. Krusch, Dissertation, University of Bonn, 1977 (unpublished).

<sup>11</sup>M. Deicher, O. Echt, E. Recknagel, and Th. Wichert, *Hyp.*

*Int.* **10**, 667 (1981).

<sup>12</sup>M. I. Baskes, C. L. Bisson, and W. D. Wilson, *J. Nucl. Mater.* **83**, 139 (1979).

<sup>13</sup>S. E. Donnelly and C. J. Rossouw, *Science* **230**, 1272 (1985). See also C. J. Rossouw and S. E. Donnelly, *Phys. Rev. Lett.* **55**, 2960 (1985).

<sup>14</sup>H. de Waard, F. Pleiter, D. O. Boerma, L. Niesen, and G. L. Zhang, *Nucl. Instrum. Methods* **209/210**, 899 (1983).

<sup>15</sup>G. Schatz, T. Klas, R. Platzer, J. Voigt, and R. Wesche, *Hyp. Int.* **34**, 555 (1987).

<sup>16</sup>F. Pleiter (private communication).

<sup>17</sup>F. Pleiter, K. Post, M. Mohsen, and T. S. Wierenga, *Phys. Lett.* **101A**, 363 (1984).

<sup>18</sup>M. Deicher, G. Grübel, E. Recknagel, W. Reiner, and Th. Wichert, *Mater. Sci. Eng.* **69**, 57 (1985).